Computer Methods in Biomechanics and Biomedical Engineering
Vol. 13, No. 2, April 2010, 171–183

Taylor & Francis
Taylor & Francis Group

A computationally efficient optimisation-based method for parameter identification of kinematically determinate and over-determinate biomechanical systems

M.S. Andersen[a]*, M. Damsgaard[b], B. MacWilliams[c] and J. Rasmussen[a]

[a]*Department of Mechanical Engineering, Aalborg University, Pontoppidanstraede 101, DK-9220 Aalborg East, Denmark;* [b]*AnyBody Technology A/S, Aalborg, Denmark;* [c]*Shriners Hospital for Children, Salt Lake City, UT, USA*

(*Received 26 February 2009; final version received 26 May 2009*)

This paper introduces a general optimisation-based method for identification of biomechanically relevant parameters in kinematically determinate and over-determinate systems from a given motion. The method is designed to find a set of parameters that is constant over the time frame of interest as well as the time-varying system coordinates, and it is particularly relevant for biomechanical motion analysis where the system parameters can be difficult to accurately determine by direct measurements. Although the parameter identification problem results in a large-scale optimisation problem, we show that, due to a special structure in the linearised Karush–Kuhn–Tucker optimality conditions, the solution can be found very efficiently. The method is applied to a set of test problems relevant for gait analysis. These involve determining the local coordinates of markers placed on the model, segment lengths and joint axes of rotation from both gait and range of motion experiments.

Keywords: parameter identification; kinematic analysis; motion capture; range of motion; gait

Introduction

Identification of kinematical model parameters, e.g. local marker coordinates, segment lengths and joint rotation axes, is necessary when performing kinematic analysis of biomechanical systems from motion capture data. In order to determine these parameters, three different basic approaches have been reported in the literature, i.e. anatomical landmarks, functional and optimisation. Anatomical landmark methods use palpation of bony landmarks to identify the segment and joint parameters using experimentally determined relationships between these (Bell et al. 1990; Davis et al. 1991; Vaughan et al. 1992). Functional methods work by identifying a simple kinematical model from the motion between two segments. Typically, this method is used to identify the hip joint centre by fitting a sphere to the motion of the thigh with respect to the pelvis and the hip joint centre is determined to be in the centre of the identified sphere (Persson et al. 1995; Leardini et al. 1999). Finally, optimisation methods have been used to identify model parameters for models of single joints (Bogert et al. 1994), a model of a human leg and pelvis (Reinbolt et al. 2005), a lower extremity model (Charlton et al. 2004) and full body models (Fregly et al. 2007; Reinbolt et al. 2008). Charlton et al. (2004) and Reinbolt et al. (2005) used a two-level optimisation method which involves decomposing the problem into two embedded optimisation problems. The outer layer adjusts the model parameters and the inner layer determines the motion of the model given the current model parameters. This algorithm is run until a given objective function is minimised, typically the least-square difference between measured marker trajectories and the corresponding point in the model. Reinbolt et al. (2005) used a particle swarm global optimisation method for the outer layer and a local optimisation method for the inner layer. Additionally, the method by Reinbolt et al. (2005) was formulated for models described using generalised coordinates only which leads to unconstrained optimisation problems. One of the main problems with this approach is the large need for computational power, which Reinbolt et al. (2005) addressed using a cluster supercomputer environment.

To overcome this problem, Fregly et al. (2007) and Reinbolt et al. (2008) recently proposed to describe the trajectories of the system coordinates using polynomials or B-splines and used the control parameters of these functions as unknown constant parameters in the optimisation problem instead of the system coordinates. While this eliminates the need for an inner layer in the optimisation problem, and hereby reduces the computational requirements, it introduces two new issues. The first is that it is now necessary to determine how many control parameters are required to allow sufficient motion capabilities of the analysed mechanism, which may not always be a trivial task. The other is that if a non-minimal set of system coordinates is used, where the system

*Corresponding author. Email: msa@me.aau.dk

ISSN 1025-5842 print/ISSN 1476-8259 online

DOI: 10.1080/10255840903067080
http://www.informaworld.com

coordinates are dependent, for instance Euler parameters used to describe orientations, it may be difficult to ensure that the required constraint(s) on these coordinates are satisfied sufficiently accurately.

Ideally, rather than introducing these approximations to the original challenging, large-scale optimisation problem, methods should be developed which explore all structure in the problem to derive a computationally efficient solution algorithm. For other challenging large-scale optimisation problems, especially convex problems, utilisation of problem structure has been very successful [see for instance Boyd and Vandenberghe (2004) for examples].

Therefore, in this paper, we shall provide a computationally efficient, local optimisation-based method for parameter identification of a general class of determinate and over-determinate mechanical systems from a given motion input. The problem formulation we propose allows model specifications using both a minimal and non-minimal sets of system coordinates as well as side constraints on the model parameters. This leads to a large-scale nonlinear and non-convex constrained optimisation problem. Hereafter, we show that a local minimiser can be found efficiently due to a special structure in the linearised Karush–Kuhn–Tucker (KKT) first-order optimality conditions. Although the method can easily be turned into a global optimisation method by starting the local optimisation method from multiple initial conditions, we focus our attention on solving the local optimisation problem as efficiently as possible. It should be noted that when a model is formulated using a minimal set of generalised coordinates and there are no constraints on the constant model parameters, the optimisation problem that we propose here and that of Reinbolt et al. (2005) will lead to identical solutions.

Methods

A mechanical system that is subject to holonomic constraints can be formulated as a set of m equations of the n_q-dimensional time-dependent system coordinates, $q(t)$, n_d-dimensional model constants, d, and time, t (Nikravesh 1988; Andersen et al. 2008):

$$\Gamma(q(t), d, t) = 0. \tag{1}$$

Depending on the number of coordinates and the number of equations, these equations can either be under-determinate ($m < n_q$), determinate ($m = n_q$) or over-determinate ($m > n_q$). Under-determinate biomechanical systems have so far not been treated generally because the equations will always have infinitely many solutions and pertinent approaches are problem specific. Determinate systems have been well studied and standard solution methods exist for this case (Nikravesh 1988). Over-determinate systems have received some treatment over the past decade because this situation happens frequently when the motion of a rigid-body model is estimated from a motion capture experiment (Lu and O'Connor 1999; Ausejo et al. 2006; Andersen et al. 2008). In this paper, we shall focus on determinate and over-determinate systems and we shall adopt the notation from Andersen et al. (2008).

Since over-determinacy means that there generally does not exist a solution to Equation (1), some re-arrangement of the equations is required in order to define what constitutes a solution. Andersen et al. (2008) introduced the concept of having the equations split into two sets: (1) $\Psi(q(t), d, t)$ a set of equations that only has to be solved 'as well as possible' in some sense, and (2) $\Phi(q(t), d, t)$ a set of equations that has to be solved exactly:

$$\Gamma(q(t), d, t) = \begin{bmatrix} \Psi(q(t), d, t) \\ \Phi(q(t), d, t) \end{bmatrix}. \tag{2}$$

This split of the equations into these two sets can be done in any way as long as the solution set of $\Phi(q(t), d, t) = 0$ is non-empty. Typically, $\Psi(q(t), d, t)$ consist of the marker constraints, i.e. equations that specify that the marker position in the model must be equal to the measured position, whereas $\Phi(q(t), d, t)$ contain the joint constraints of the kinematical system.

Over-determinate kinematics

We shall start off by assuming that the constant model parameters are known and denote them by $\hat{d}$. If it is desired to solve Equation (2) at N discrete time steps,

$$q_1 = q(t_1), \quad q_2 = q(t_2), \ldots, q_N = q(t_N), \tag{3}$$

the solution can be found by solving the following nonlinear and non-convex optimisation problem (Andersen et al. 2008):

$$\begin{aligned} q_i^* = \ & \arg\min_{q_i} G(\Psi(q_i, \hat{d}, t_i)) \\ & \text{s.t.} \quad \Phi(q_i, \hat{d}, t_i) = 0 \end{aligned} \tag{4}$$

for $i = 1, 2, \ldots, N$. The scalar objective function, $G(\Psi(q_i, \hat{d}, t_i))$, has been introduced to express how violations of the $\Psi(q_i, \hat{d}, t_i)$ equations are allowed. Ausejo et al. (2006) and Andersen et al. (2008) demonstrated the use of a weighted least-square objective function:

$$G(\Psi(q_i, \hat{d}, t_i)) = \frac{1}{2}\Psi(q_i, \hat{d}, t_i)^T W(t_i) \Psi(q_i, \hat{d}, t_i) \tag{5}$$

for lower extremity gait analysis and upper extremity car driving, respectively. In this paper, we shall not assume

any particular form of G while the equations for determination of the optimal constant model parameters are derived. The only requirement is that G is twice differentiable with respect to both q and d.

Before formulating an optimisation problem that can be used to find the constant model parameters, we shall first review the KKT conditions and linearised KKT conditions for the problem in Equation (4) as these equations will re-appear later and play a key role in deriving an efficient algorithm for finding the solution. Notice that these conditions addresses a single time frame, i.

The KKT conditions for the optimisation problem in Equation (4) are (refer for instance Boyd and Vandenberghe (2004)):

$$\begin{aligned} G_{q_i}^T + \Phi_{q_i}^T \lambda_i &= 0, \\ \Phi &= 0, \end{aligned} \tag{6}$$

where the subscript, q_i, denotes the partial derivative with respect to q_i and λ_i is a vector of Lagrange multipliers. The optimality conditions for a constrained optimisation problem basically state that the partial derivatives of the objective function at a local minimiser has to be a linear combination of the partial derivatives of the constraint equations. Moreover, the solution point has to be feasible (i.e. has to satisfy the constraints).

When a Newton-based method (Boyd and Vandenberghe 2004) is used to find a local minimiser, the linearised KKT conditions are required:

$$\begin{bmatrix} G_{q_i q_i}^T + (\Phi_{q_i}^T \lambda_i)_{q_i} & \Phi_{q_i}^T \\ \Phi_{q_i} & 0 \end{bmatrix} \begin{bmatrix} \Delta q_i \\ \Delta \lambda_i \end{bmatrix} = \begin{bmatrix} -G_{q_i}^T - \Phi_{q_i}^T \lambda_i \\ -\Phi \end{bmatrix}, \tag{7}$$

where Δq_i and $\Delta \lambda_i$ denote the search direction at step i, which is found by solving the linear set of equations in Equation (7). For well-conditioned systems, the matrix on the left hand side will be invertible (Andersen et al. 2008); this will be exploited later.

Constant parameter determination

In this section, we shall first formulate a large-scale optimisation problem that ties all the samples together such that the optimal constant parameters, d^*, can be determined. Secondly, we shall derive an efficient algorithm for solving this optimisation problem.

If we assume that the optimal constant parameters, d^*, are known, we know that the optimal system coordinates at time step i, q_i^*, can be found by solving the optimisation problem in Equation (4). Now we seek an optimisation problem whose solution would produce the same optimal system coordinates for each time step and optimal constant parameters over all the time steps. One such optimisation problem could be to simply sum all the individual objective functions in Equation (4) over the whole time period as well as specifying the subject to constraints for all time steps:

$$\begin{aligned} \min_{q(t_1), q(t_2), \ldots, q(t_N), d} \quad & H(G_1, G_2, \ldots, G_N) = \sum_{i=1}^{N} G(\Psi(q(t_i), d, t_i)) \\ \text{s.t.} \quad & \Phi(q(t_k), d, t_k) = 0 \end{aligned} \tag{8}$$

for $k = 1, 2, \ldots, N$. That this optimisation problem has the desired property, we shall prove by contradiction. First, assume that the global optimising set of system coordinates, q_i^*, and constant parameters, d^*, for the problem in Equation (4) are known. This set of parameters would be feasible for the optimisation problem in Equation (8) and would result in an objective function value:

$$H_1 = \sum_{i=1}^{N} G(\Psi(q_i^*, d^*, t_i)). \tag{9}$$

Now, assume existence of another set of feasible system coordinates, q_i', and constant parameters, d', that force the optimisation problem in Equation (8) to attain its global minimum:

$$H^* = \sum_{i=1}^{N} G(\Psi(q_i', d', t_i)). \tag{10}$$

Since H^* is assumed to be the global minimiser of the optimisation problem in Equation (8), it means that $H^* \leq H_1$. If the inequality sign applies, it means that there exists a third set of feasible system coordinates and constant parameters that can lower the value of H_1. However, since H is constructed as a linear combination of the objective function values for each time step, the only way to reduce its value is to reduce one or more of the individual objective function values. However, that this should be possible contradicts the original assumption that q_i^* and d^* are global minimisers for each individual objective function and, hence, $H^* = H_1$, implying that $q_i^* = q_i'$ and $d^* = d'$ if it is assumed that the optimisation problem has a unique global optimiser.

Before proceeding to derive an algorithm for the solution of Equation (8), we shall modify it slightly by adding a constraint equation to the problem that is only function of the constant parameters. Although these could in principle be comprised in the $\Phi(q(t), d, t) = 0$ set, there are advantages in treating them separately as we shall see later.

Therefore, the optimisation problem we wish to solve is:

$$\begin{aligned} \min_{q(t_1), q(t_2), \ldots, q(t_N), d} \quad & \sum_{i=1}^{N} G(\Psi(q(t_i), d, t_i)) \\ \text{s.t.} \quad & \Phi(q(t_k), d, t_k) = 0, \\ & T(d) = 0 \end{aligned} \tag{11}$$

for $k = 1, 2, \ldots, N$.

A basic two-step iterative scheme for solving an optimisation problem like the one in Equation (11) involves: (1) Calculate a search direction along which a step will bring us closer to the solution. 2) Select a step length in the selected search direction. In this paper, we shall focus our attention on step (1) as it is the most challenging for a large-scale problem. For step (2), we shall apply a simple backtracking line-search (Boyd and Vandenberghe 2004).

We shall use a Newton-based method (Boyd and Vandenberghe 2004) to find a local minimiser of the optimisation problem in Equation (11). To this end, the KKT conditions must be derived and solved. Additionally, the linearised KKT conditions must be derived, which result in a linear set of equations. The large number of variables in the optimisation problem makes this linear set of equations large and requires careful consideration of the numerical procedure to find the solution.

In the interest of compactness of the equations, we shall define the following shorter notation for the objective function at timestep, k, ${}^kG \equiv G(\Psi(q(t_k), d, t_k))$, and for the constraint equations, ${}^k\Phi \equiv \Phi(q(t_k), d, t_k)$. The first step towards deriving the KKT conditions is to define the so-called Lagrange function, which is given as the objective function plus all constraint equations, each multiplied by an associated Lagrange multiplier (Boyd and Vandenberghe 2004):

$$L = \sum_{k=1}^{N} {}^kG + \sum_{k=1}^{N} {}^k\Phi^T \lambda_k + T^T \nu, \tag{12}$$

λ_k are the Lagrange multipliers associated with the constraints evaluated at time step k and ν the Lagrange multipliers for the T constraints. The KKT conditions are then derived by differentiation of L with respect to all design variables and Lagrange multipliers and equating all the equations to zero:

$$\begin{aligned} L_{q_i} &= {}^iG_{q_i}^T + {}^i\Phi_{q_i}^T \lambda_i = 0, \\ L_d &= \sum_{k=1}^{N} {}^kG_d^T + \sum_{k=1}^{N} {}^k\Phi_d^T \lambda_k + T_d^T \nu = 0, \\ L_{\lambda_i} &= {}^k\Phi = 0, \\ \mathrm{L}_\nu &= T = 0, \end{aligned} \tag{13}$$

for $i = 1, 2, \ldots, N$.

Before writing out the linearised KKT conditions, which are obtained by performing a first-order Tayler expansion of Equation (13), we shall define a few vectors and matrices to achieve a more compact form of the equations:

$$\begin{aligned} A_i &\equiv \begin{bmatrix} {}^iG_{q_iq_i}^T + \left({}^i\Phi_{q_i}^T \lambda_i\right)_{q_i} & {}^i\Phi_{q_i}^T \\ {}^i\Phi_{q_i} & 0 \end{bmatrix}, \\ B_i &\equiv \begin{bmatrix} {}^iG_{dq_i}^T + \left({}^i\Phi_d^T \lambda_i\right)_{q_i} & {}^i\Phi_d^T \end{bmatrix}, \\ C &\equiv \left[\sum_{k=1}^{N} \left({}^kG_{dd}^T + \left({}^k\Phi_d^T \lambda_i\right)_d \right) + \left(T_d^T \nu\right)_d \right], \\ D &\equiv T_d, \\ a_i &\equiv \begin{bmatrix} {}^iG_{q_i}^T + {}^i\Phi_{q_i}^T \lambda_i \\ {}^i\Phi \end{bmatrix}, \\ b &\equiv \left[\sum_{k=1}^{N} \left({}^kG_d^T + {}^k\Phi_d^T \lambda_i \right) + T_d^T \nu \right], \\ c &\equiv T. \end{aligned} \tag{14}$$

With these definitions, the linearised KKT conditions can be written on the following compact matrix form:

$$\begin{bmatrix} A_1 & 0 & \cdots & \cdots & 0 & B_1^T & 0 \\ 0 & A_2 & 0 & \cdots & 0 & B_2^T & 0 \\ 0 & 0 & \ddots & 0 & 0 & \vdots & \vdots \\ 0 & \vdots & 0 & \ddots & 0 & \vdots & \vdots \\ 0 & 0 & 0 & 0 & A_N & B_N^T & 0 \\ B_1 & B_2 & \cdots & \cdots & B_N & C & D^T \\ 0 & 0 & \cdots & \cdots & 0 & D & 0 \end{bmatrix} \begin{bmatrix} \begin{bmatrix} \Delta q_1 \\ \Delta \lambda_1 \end{bmatrix} \\ \begin{bmatrix} \Delta q_2 \\ \Delta \lambda_2 \end{bmatrix} \\ \vdots \\ \begin{bmatrix} \Delta q_N \\ \Delta \lambda_N \end{bmatrix} \\ \Delta d \\ \Delta \nu \end{bmatrix} = \begin{bmatrix} -a_1 \\ -a_2 \\ \vdots \\ -a_N \\ -b \\ -c \end{bmatrix}. \tag{15}$$

Even for small-scale mechanical systems, this linear set of equations will be too large to solve directly due to all the zero elements that are in the matrix if handled in dense format. Therefore, an alternative approach is needed which should utilise all the structure in the equations.

One alternative is sparse matrix representations. However, since this linear set of equations will have the same structure no matter which mechanical system is analysed, the structure can be utilised directly in the solution algorithm rather than online.

The main thing to notice about this matrix is that the A_i matrices on the diagonal in the sub-matrix in the upper left hand corner are the same matrices as the coefficient matrix in Equation (7). For well-conditioned systems, these matrices will be invertible. This means that in the top most N equations, Δq_i and $\Delta\lambda_i$ can be isolated:

$$\begin{aligned} & A_i \begin{bmatrix} \Delta q_i \\ \Delta\lambda_i \end{bmatrix} + B_i^T \Delta d = -a_i \\ & \Updownarrow \\ & \begin{bmatrix} \Delta q_i \\ \Delta\lambda_i \end{bmatrix} = -A_i^{-1} a_i - A_i^{-1} B_i^T \Delta d. \end{aligned} \tag{16}$$

If these equations are substituted into the second last equation in Equation (15), a much smaller linear set of equations with only Δp and $\Delta\nu$ is obtained:

$$\begin{bmatrix} -\sum_{k=1}^{N} B_k A_k^{-1} B_k^T + C & D^T \\ D & 0 \end{bmatrix} \begin{bmatrix} \Delta d \\ \Delta\nu \end{bmatrix} = \begin{bmatrix} -b + \sum_{k=1}^{N} B_i A_i^{-1} a_i \\ -c \end{bmatrix}. \tag{17}$$

Hereby, the solution to the large linear set of equations in Equation (15) can be found by first solving the much smaller linear set of equations in Equation (17) and thereafter substitute the found Δp into Equation (16) for all time steps to find Δq_i and $\Delta\lambda_i$ for $i = 1, 2, \ldots, N$.

Solution algorithm

Given the above method for finding a suitable search direction, it is now possible to write out a full solution algorithm to solve Equation (13) by using the search direction calculated from Equations (16) and (17). However, in order to start a local minimisation algorithm, an initial guess is required for both q_i and d for all $i = 1, 2, \ldots, N$. The properties in general and the nonlinearity of the problem in particular makes this a challenging task for a user of a biomechanical simulation system, so some method is needed to derive this initial guess. We shall assume that the initial guess on the constant parameters is sufficiently good, implying that these have been estimated fairly accurately by the user, e.g. based on traditional direct measurements on the subject. Thus, it is possible to keep the constant parameters fixed and then solve the optimisation problem in Equation (4) to find an initial guess on the system coordinates at all samples given an initial guess on the system coordinates at the first time step. While finding the initial guess, the $T(d) = 0$ equations are neglected. Hereby, a solution algorithm can be written out as follows:

(1) Specify an initial guess for the system coordinates at the first sample, $\hat{q}_1^0$, and an initial guess on the constant parameters p^0.
(2) Solve the optimisation problem in Equation (4) to find a new set of initial system coordinates to be used when solving the optimisation problem in Equation (11), $q_1^0, q_2^0, \ldots, q_N^0$.
(3) Solve the optimisation problem in Equation (11):
    (a) Initialise the iteration counter, $k \coloneqq 1$, and set the initial conditions $q_i^k \coloneqq q_i^0$ and $d^k \coloneqq d^0$ for $i = 1, 2, \ldots, N$.
    (b) Check if the KKT conditions in Equation (13) are satisfied and if yes break and return the result else go to (c).
    (c) Calculate the search direction, Δq_i, $\Delta\lambda_i$, Δd and $\Delta\nu$, by first solving Equation (17) and substitute the results into Equation (16), for $i = 1, 2, \ldots, N$.
    (d) Calculate a step length, γ, using a backtracking line search (Boyd and Vandenberghe 2004).
    (e) Update the variables:

$$\begin{aligned} q_i^{k+1} &\coloneqq q_i^k + \gamma\Delta q_i, \\ \lambda_i^{k+1} &\coloneqq \lambda_i^k + \gamma\Delta\lambda_i, \\ d^{k+1} &\coloneqq d^k + \gamma\Delta d, \\ \nu^{k+1} &\coloneqq \nu^k + \gamma\Delta\nu. \end{aligned}$$

    (f) Update the iteration counter $k \coloneqq k + 1$ and go to (b).

Implementation

Before implementing the above algorithm, one computational issue should be considered. Both Equations (16) and (17) contain the product between the inverse of the A_i matrices and a vector ($A_i^{-1} a_i$) and a matrix ($A_i^{-1} B_i^T$). Rather than first calculating the computationally expensive inverse of A_i and then multiplying it with the vector and the matrix, the A_i matrices should be factorised and afterwards each column of the matrix (and the one column of the vector) should be forward-backward substituted. This approach will be much less computationally expensive. Also, since these terms appear in both Equations (16) and (17) it is only necessary to calculate them once per time step.

The method has been implemented generally in C++ where the model interface consists of evaluating the $\Phi(q(t), d, t)$ and $\Psi(q(t), d, t)$ functions and all the required derivatives of these. The model equations and derivatives are implemented using an automatic differentiation package developed particularly for this purpose.

Example and results

The above optimisation algorithm has been applied to the kinematic analysis of gait and range of motion (ROM) for a healthy subject. The problem that we consider here consists of morphing a cadaver model into a model of a subject by means of segment scaling laws, joint rotation axes and local marker coordinate optimisation. This is a classical problem in musculoskeletal modelling where a base model with muscle attachment points, muscle properties, joint locations, etc. has been determined from a cadaver. Hereafter, motion information for a subject is collected using motion capture and it is desired to impose the measured motion on the model. In order to achieve this, scaling laws have to be defined such that the cadaver model can be morphed to the same size and shape as the subject from whom the motion was captured, the local coordinates of the marker placements on the model have to be found and the joint rotation axes have to be altered to fit the subject as well as possible. Common for all these properties is that they are constant over the whole measurement trial and can therefore be determined using the algorithm we described in this paper together with the motion of the model.

Experimental procedure

Two motion capture experiments were performed on a single subject at the Motion Analysis Laboratory at Shriners Hospital for Children, Salt Lake City, UT, USA. The first of these was normal walking at a self-selected pace along a straight walkway and the other was a full ROM experiment for the lower extremities. Markers were placed on pelvis, the thighs, shanks, and feet as outlined in Table 1. The markers were recorded at 100 Hz using a Vicon motion capture system (Vicon, Centennial, CO, USA). The subject was holding onto a wooden pole while performing ROM. In the ROM experiment, the subject was instructed to move all joint degrees-of-freedom (dof) to their maximum one at a time in the order left foot inversion/eversion, plantar flexion/extension, knee flexion/extension and hip abduction/adduction, flexion/extension and internal/external rotation and hereafter the whole experiment was repeated for the right leg. The whole trial took about 47 s. After the motion capture session, the marker trajectories were low-pass filtered using a second-order, zero-phase, Butterworth filter with a cut-off frequency of 10 Hz. During the ROM trial, some markers were occluded a couple of times. In order to handle this, weight functions were created using the method of Andersen et al. (2007) for each marker. It assigns a weight of one when a marker is visible and a weight of zero when it is not. Even when some markers were missing, the redundancy of the marker configuration secured enough information to recover the motion at all times, rendering interpolation of marker trajectories unnecessary.

Model description

The model we shall use to demonstrate the method is an 18 dof lower extremity model consisting of the pelvis, femur, tibia, talus and rigid feet segments (Figure 1). The base

Table 1. The marker placements as well as which markers are optimised.

Marker name	Placement	Optimised *x*-coordinate	Optimised *y*-coordinate	Optimised *z*-coordinate
RPSIS	Pelvis	Yes	No	Yes
LPSIS	Pelvis	Yes	No	Yes
LASIS	Pelvis	No	No	No
RASIS	Pelvis	No	No	No
LLATKNEE	Left thigh	No	No	No
LLATANKLE	Left shank	No	No	No
LMEDANKLE	Left shank	Yes	Yes	Yes
LTOE	Left foot	Yes	Yes	Yes
LFIRSTMT	Left foot	No	No	No
LFIFTHMT	Left foot	No	No	No
LHEEL	Left foot	Yes	Yes	Yes
RLATKNEE	Right thigh	No	No	No
RLATANKLE	Right shank	No	No	No
RMEDANKLE	Right shank	Yes	Yes	Yes
RTOE	Right foot	Yes	Yes	Yes
RFIRSTMT	Right foot	No	No	No
RFIFTHMT	Right foot	No	No	No
RHEEL	Right foot	Yes	Yes	Yes

A 'Yes' means that the marker coordinate is optimised and a 'No' means that it is not.

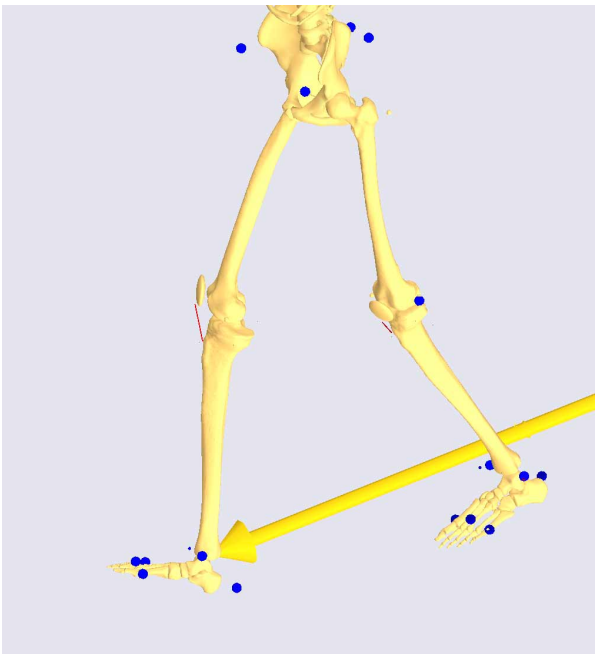

Figure 1. The lower extremity model and its optical marker placements.

model is based on the morphological data set for the lower extremities by Klein Horsman et al. (2007). In this model, the hips are modelled as spherical joints, the knees, ankles and subtalar joints are modelled as revolute joints. The model is described using a full Cartesian formulation, where the system coordinates is a collection of the global positions and orientations of all segments. As rotational coordinates, we use Euler parameters (Nikravesh 1988). The equations specifying the vector difference between the measured marker trajectories and the corresponding points in the model in global coordinates are assigned to $\Psi(q(t), d, t)$, whereas all joint constraint as well as the constraints on the Euler parameters are assigned to $\Phi(q(t), d, t)$. For a detailed description of how to define a model using a full Cartesian formulation, please see Andersen et al. (2008).

Since the base model already prescribes the definition of the local coordinate systems of the segments, the markers in the motion capture experiment have to be defined in the same coordinate system on the model. To achieve this, a few of the markers were placed on bony landmarks on the model bone geometry while the rest were treated as unknown constant model parameters and optimised. In Table 1, the placement of markers can be seen as well as which markers were optimised and which were not. Generally, enough markers have to be fixed on the skeleton to define all dof, i.e. in this case at least 18. On top of this, markers also have to be fixed to ensure that the segment lengths and joint axes are well defined. For instance, if all markers were considered unknown, the optimisation problem would be ill posed and have infinitively many solutions. If, for instance, all markers on pelvis were considered unknown, then any arbitrary offset on the tilt of pelvis would create an equally good solution. Besides the marker coordinates, the segment lengths and the joint rotation axes were also optimised. How many of these constant parameters that can be optimised depend on the motion that the subject performs. A full list of the model parameters that were optimised can be seen in Table 2. Segment scaling was defined in the simplest possible sense where each segment is scaled uniformly in all directions using only one parameter per segment. This scaling law affects the location of the joint centres as well as the position of both the optimised and fixed markers on the skeleton. Although this is a simplistic scaling model, it ensures that, after optimisation, the location of all muscle attachment points on the bones are also known since these are scaled in the same manner. Alternative scaling laws could also have been used. For instance, by scaling differently in all three directions, using also the segment masses in the law (Rasmussen et al. 2005), or even allow not only linear stretching of the segments but also bending. Please notice that the hip joint centres in the pelvis segment were only altered indirectly by the applied scaling law. The joint rotation axes were defined as a constantly oriented coordinate system with respect to the corresponding segment defined using Cardan angles, where the first rotation component is kept constant (i.e. the z-axis for all joints). Since the rotation axes for all the joints are defined for both segments that the joint connects, only the axes given on one of these were optimised. For the knees, the joint axes in the thigh coordinate system, for the ankle joint, the joint axes in the shank coordinate system, and for the subtalar joint, the joint axes in talus' coordinate system are optimised. The Cardan angle sequences defined in the model are x-y-z for the knees, and y-x-z for the ankle and subtalar joints.

Table 2. The table shows the segment lengths and joint axes that are optimised from the gait and ROM trials.

Trial	Parameter
Gait and ROM	Pelvis width Left and right thigh length Left and right shank length Left and right foot length Left and right knee axes
ROM	Left and right subtalar joint axes Left and right ankle joint axes

The basic idea utilised to pick which markers to fix to the bone geometry was to identify the markers which should define the different segment lengths and joint axes. For pelvis, we chose to use the ASIS markers to define the pelvis width as well as the y-coordinate of the PSI markers to define the pelvis tilt. To define the thigh

length, we used the knee marker, and to define the shank length as well as the knee joint axes, we used the lateral ankle marker. In addition, these also define the joint coordinates of the hip and knee. For the feet, the markers on the first and fifth metatarsal were fixed which defines the length of the foot, the ankle and subtalar joint axes as well as the joint coordinates for these same joints. Unfortunately, this approach also means that the identified mechanism will be sensitive to inaccurate placements of these fixed markers on the bone geometry as well as differences between the test subject's and the cadaver's bone geometry.

Due to the very little motion in the ankle and subtalar joints during gait, these joint rotation axes were not optimised from the gait trial but only from the ROM trial. In the gait trial, two models were constructed; one where the ankle and subtalar joint axes were kept at the cadaver values and one where the ankle and subtalar joint axes were kept at the values found in the ROM-optimised model. After the three models have been constructed, the models were evaluated in the gait experiment by solving the optimisation problem in Equation (4). Hereafter, the mean the marker error at each time step is calculated for the models over the gait trial and can be seen in Figure 2. Additionally, the calculated segment lengths and joint rotation axes for the trials can be seen in Table 3 and the calculated local marker coordinates in Tables 4 and 5.

Results

Overall, in the gait experiment, the gait-optimised model, where the ankle and subtalar joint axes from the ROM-optimised model are used, results in the lowest mean marker error over the gait trial with a value of 5.5 ± 3.3 mm. The second lowest mean marker error is obtained with the ROM-optimised model with a value 6.1 ± 4.0 mm. Lastly, the highest mean marker error is obtained for the model optimised from the gait trial, when the ankle and subtalar joint axes from the cadaver are used, with a value 6.5 ± 4.0 mm. The time history of the mean error between the measured marker trajectories and the corresponding point in the model can be seen in Figure 2 over the gait trial for the three models.

The optimised segment lengths in the three models show notable differences (see Table 3), e.g. both the gait-optimised models find a pelvis width that is 6 mm longer than that found using the ROM data. Since a larger pelvis width scales the whole pelvis segment to be larger uniformly, shorter thigh segment lengths are required if the knee joint centre should remain at the same position

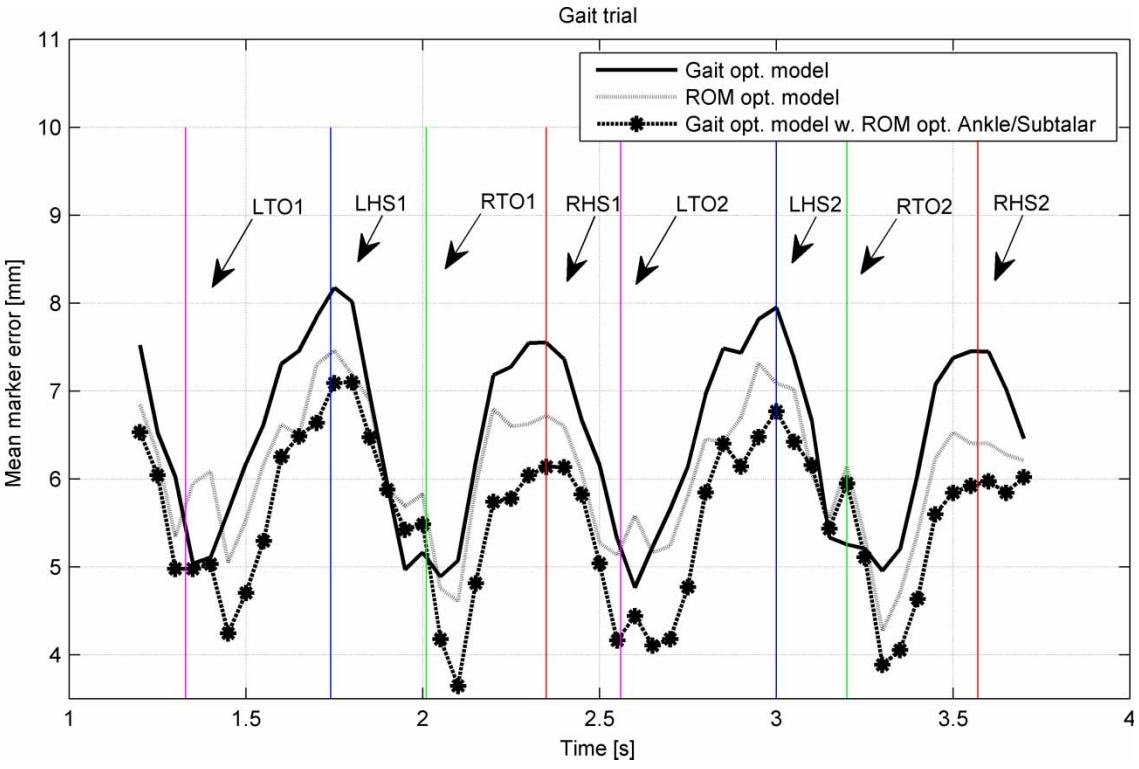

Figure 2. The mean errors between all measured markers and the corresponding points on the models over the gait trial. The vertical lines indicate gait events, e.g. RHSX indicates heel strike number X with the right foot and RTOX indicates toe off number X with the right foot. Similar indications are made for the left foot using LHSX and LTOX.

Table 3. Segment lengths and joint rotation axes after optimisation.

Variable	Gait trial	Gait trial and ROM optimised ankle and subtalar joint axes.	ROM trial
Pelvis width (m)	0.157	0.157	0.151
Left thigh length (m)	0.457	0.458	0.468
Left shank length (m)	0.495	0.497	0.500
Left foot length (m)	0.232	0.242	0.242
Right thigh length (m)	0.479	0.479	0.488
Right shank length (m)	0.494	0.495	0.498
Right foot length (m)	0.204	0.207	0.205
Left knee rot *x* (°)	9.85	14.38	13.18
Left knee rot *y* (°)	−7.62	−4.58	−28.07
Left ankle rot *x* (°)	−11.92*	−27.96**	−27.96
Left ankle rot *y* (°)	44.29*	9.34**	9.34
Left sub rot *x* (°)	−12.89*	−12.03**	−12.03
Left sub rot *y* (°)	104.97*	113.04**	113.04
Right knee rot *x* (°)	−7.73	−8.65	−10.77
Right knee rot *y* (°)	−8.19	−8.82	−8.25
Right ankle rot *x* (°)	11.92*	8.82**	8.82
Right ankle rot *y* (°)	−44.29*	11.29**	11.29
Right sub rot *x* (°)	12.89*	−16.39**	−16.39
Right sub rot *y* (°)	−104.97*	−143.98**	−143.98

The lengths are given in meters and the angles in degrees.
A '*' indicates that the variable was not optimised and retained the original (cadaver) value. A '**' indicates that the variable was not optimised in the given trial, but the value was adopted from the ROM trial.

in space. This is also what happens since the thigh lengths in both gait models are estimated to be approximately 1 cm shorter than those estimated from the ROM trial. The variation of estimated shank lengths between all models are within a few millimetres. The largest difference in segment length estimations between the three models are seen in the left foot, which is estimated to be 1 cm shorter in the gait-optimised model with the cadaver values for the ankle and subtalar joints than those estimated from the two other models. The difference in right foot length estimation between all three models is within a millimetre. The knee joint rotation axes estimation shows largest differences for the left side where the first rotation component is within 5° for the three models. However, for the second component, the two gait-optimised models are within 3° but the ROM-optimised model gives a value that is more than 20° different. For the right side, all the knee axes estimations are within 3°. The ankle and subtalar joint

Table 4. Scaled local marker coordinates from both the Gait and ROM trial after optimisation.

	Gait trial			ROM trial		
Marker name	*x* (m)	*y* (m)	*z* (m)	*x* (m)	*y* (m)	*z* (m)
RPSIS	−0.0547	−0.0070*	0.0390	−0.0594	−0.0067*	0.0380
LPSIS	−0.0582	−0.0070*	−0.0341	−0.0641	−0.0067*	−0.0337
LASIS	0.1288*	−0.0509*	−0.1399*	0.1237*	−0.0489*	−0.1343*
RASIS	0.1282*	−0.0474*	0.1430*	0.1231*	−0.0455*	0.1373*
LLATKNEE	0.0394*	−0.4513*	−0.0636*	0.0404*	−0.4623*	−0.0651*
LLATANKLE	0.0562*	−0.9937*	−0.0446*	0.0567*	−1.0051*	0.0451*
LMEDANKLE	0.1216	−0.9751	−0.0001	0.1205	−0.9856	0.0078
LTOE	0.1344	−0.8373	−0.0698	0.1410	−0.8781	−0.0743
LFIRSTMT	0.1594*	−0.8477	0.0274	0.1669*	−0.8876*	−0.0287*
LFIFTHMT	0.0964*	−0.8477*	−0.0904*	0.1009*	−0.8876*	−0.0947*
LHEEL	0.0100	−0.7403	0.0342	0.0070	−0.7786	0.0151
RLATKNEE	0.0413*	−0.4695*	0.0670*	0.0421*	−0.4781*	0.0682*
RLATANKLE	0.0561*	−0.9914*	0.0445*	0.0566*	−1.0007*	0.0449*
RMEDANKLE	0.1210	−0.9723	0.0082	0.1217	−0.9811	−0.0130
RTOE	0.1241	−0.7510	0.0683	0.1264	−0.7531	0.0683
RFIRSTMT	0.1404*	−0.7467*	0.0241*	0.1410*	−0.7501*	0.0242*
RFIFTHMT	0.0849*	−0.7467*	0.0796*	0.0853*	−0.7501*	0.0800*
RHEEL	0.0020	−0.6436	−0.0474	−0.0215	−0.6602	−0.0268

A '*' indicates that the variable was not optimised. Please note that the unscaled coordinates of markers that were not optimised were the same in both experiments.

Table 5. Scaled local marker coordinates from the gait optimised trial, where the ankle and subtalar joint axes found from the ROM trial are used.

	Gait-optimised with ROM-optimised ankle and subtalar joint axes		
Marker name	*x* (m)	*y* (m)	*z* (m)
RPSIS	−0.0549	−0.0070*	0.0390
LPSIS	−0.0585	−0.0070*	−0.0340
LASIS	0.1288*	−0.0509*	−0.1399*
RASIS	0.1282*	−0.0474*	0.1430*
LLATKNEE	0.0395*	−0.4519*	0.0636*
LLATANKLE	0.0565*	−0.9981*	0.0448*
LMEDANKLE	0.1200	−0.9773	0.0088
LTOE	0.1393	−0.8770	−0.0738
LFIRSTMT	0.1666*	−0.8859*	−0.0286*
LFIFTHMT	0.1007*	−0.8859*	−0.0945*
LHEEL	0.0098*	−0.7740	0.0172*
RLATKNEE	0.0414*	−0.4701*	0.0670*
RLATANKLE	0.0562*	−0.9942*	0.0447*
RMEDANKLE	0.1253*	−0.9722*	−0.0110*
RTOE	0.1265	−0.7629	0.0687
RFIRSTMT	0.1426*	−0.7585*	0.0245
RFIFTHMT	0.0862*	−0.7585*	0.0809*
RHEEL	−0.0164	−0.6631	−0.0284

A '*' indicates that the variable was not optimised.

rotation axes in the gait-optimised model with the cadaver values for the ankle and subtalar joints are largely different from the values found from the ROM experiment. The largest difference of approximately 39° is seen in the right subtalar rotation around the second axes. A large difference is also seen in the estimation of the first rotation component of both the left and right ankle of approximately 30°. Since the ankle and subtalar joint rotation axes were not optimised in the gait-optimised model, the cadaver values are likely not representative for the measured subject. However, although the ankle and subtalar joint axes are largely different, only a relatively small difference is seen in the objective function value when the models are used for gait analysis. The reason for this is that there is little motion about these axes during gait and their locations are therefore less significant to the objective function value.

The optimised local marker coordinates show some differences between the models. However, most of these differences arise due to different segment scaling in the models and therefore the local marker coordinates have to be changed to continue to follow the measured marker trajectories well.

The optimisation of the model from the gait trial with only 255 samples required a few minutes of computational time on a 1.7 GHz laptop with 512 MB RAM to solve the KKT conditions with an error tolerance of 10^{-12}. For the two gait-optimised models, the optimisation problem has 16,098 total design variables (33 related to the model constants and 16,065 related to the model coordinates). On the contrary, although the optimisation from the ROM trial with 4680 samples only required 21 iterations, it took approximately 5 h to complete. The majority of this time was spent on calculating the search direction, i.e. in step 3(c) in the algorithm. This optimisation problem has 294,881 total design variables (41 related to the model constants and 294,840 related to the model coordinates).

Discussion and conclusion

In this paper, we introduced a computationally efficient local optimisation-based method for parameter estimation for determinate and over-determinate mechanical systems subject to holonomic constraints. The method was formulated such that the mechanical system of interest can both be described using a minimal and non-minimal set of system coordinates. The optimisation problem was formulated such that the sum of a function, describing how constraint violations are allowed, evaluated at all time steps of interest is minimised. Even for small-scale mechanical systems, this results in a large-scale optimisation problem that can easily have hundreds of thousands of design variables.

Hereafter, we showed that a local minimiser for the large-scale optimisation problem can be found efficiently due to a special structure in the linearised KKT conditions such that, rather than having to solve a large set of linear equations to find a search direction, it can be found by solving a series of much small linear sets of equations.

The method was demonstrated on a biomechanical problem, where it was desired to scale a base model to that of a subject by estimating the segment lengths, joint axes of rotation and local coordinates of markers placed on a model from both a gait and ROM trial. For gait analysis, the results show that the smallest error between the measured marker trajectories and the corresponding points on the model is found where the model is optimised from the gait trial, but with the joint axes of rotation for both the ankle and subtalar joints set to those found from the ROM trial. Generally, the differences in the estimated segment lengths are well within the errors in the measured marker trajectories from the motion capture experiment that must be attributed to soft tissue artefacts (STA). STA in the order of 3 cm have been reported for markers placed on the thigh and 2 cm for markers placed on the shank [see, e.g. Stagni et al. (2005) for a recent study or Leardini et al. (2005) for a review]. However, since the true segment lengths for the subject are not known, it is not possible to determine which of the results is correct.

During testing of the algorithm, synthetic motion data were generated using simple linkages with idealised joints between the segments to verify that the algorithm could recover the known model under ideal circumstances. These tests were successful. However, these tests did not

replicate the true nature of the problem and modelling of the true problem is not immediately possible. First of all, in a realistic simulation test setup, the model used to replicate the experiment must contain accurate and realistic models of the human joint anatomy, which are not yet available. Secondly, this model must also contain a realistic noise model both of instrumentation noise as well as STA. Among others, Lu and O'Connor (1999) and Reinbolt et al. (2005) assumed random or sinusoidal noise models, which must be considered over-simplifications of the complex behaviour of STA, which have been reported in the literature. Before realistic simulation setups can be made, these two issues must be adequately solved.

When the ankle and subtalar joint axes were kept at the cadaver values in the model and the rest of the model optimised from the gait trial, the foot length estimations were notably different from those found using the ROM trial. However, when the ROM-optimised ankle and subtalar joint axes were used instead of the cadaver values, the foot length estimations became close to identical. These differences in the placement of the ankle and subtalar joint axes are also the main contributors to the differences in the mean marker errors in the different models. This is because the fixed joint axes in the ankle and subtalar joints in the gait-optimised model prevents the optimiser from obtaining as good a fit for the markers on the feet as in the ROM experiment. From the point-of-view of reducing these marker errors, optimisation of the ankle and subtalar joint axes could have been included in the gait-optimised models. However, due to the very little motion around these axes, there would be no guarantee of a realistic result.

The largest differences between the gait- and ROM-optimised models are seen in the estimation of the knee joint rotation axes. The reason for this can be that the knee does not behave as a perfect revolute joint; it has been shown that both translations and rotations around all three axes occur in the knee during walking for healthy subjects (Benoit et al. 2006). Therefore, the optimised knee joint rotation axes will be placed such that the model after optimisation is capable of reproducing as much as possible of the real motion while still fulfilling the imposed constraint. For instance, if both flexion/extension and internal/external rotation occur over the trial, the optimised joint axes will be placed such that the model is capable of doing both. In that respect, the solution found by the algorithm represents the best possible fit of the model to the measured motion. Another issue is that the feet are not two-segment mechanisms with two perfect revolute joints as the model presumes. In fact, it has been shown that the feet behave differently under loading than they do unloaded (Bogert et al. 1994). Therefore, although the ankle and subtalar axes determined from the ROM trial, where the feet are unloaded when plantar flexion/extension and inversion/eversion are performed, are within the ranges normally reported for these axes, it is not certain that the estimated axes are the best possible when the foot is loaded during gait. In this study, the subtalar joint axes relative to the model foot geometry were the same as for the cadaver by construction, i.e. the relative placement of the subtalar joint axes in the foot coordinate system was not optimised. The ankle derivations and inclinations were determined to be $-5°$ and $9°$ for the left foot, respectively. An ankle derivation of $-10°$ and inclination of $21°$ were found for the right leg. Derivation and inclination of the joint axes were defined similarly to Bogert et al. (1994), which reported ankle derivations of $1.0° \pm 15.1°$ and ankle inclinations of $4.6° \pm 7.4°$ found using a 12 parameter ankle and subtalar joint model for 14 subjects.

An issue with the presented method is the possibility of local minimisers in the optimisation problem. However, from our experience, these local minimisers are easily distinguishable from the global minimiser. From the lower extremity model, we have found that there is one solution to the KKT conditions in Equation (13) that ensures that all markers are as close as possible to the measured markers. All other solutions, we have found, turn out to be saddle points, where one or more of the segments are moving such that the markers on the model are as far away from the measured markers as possible while other segments are as close as possible. A good example of this is that one of the feet can be rotated such that it is pointing away from the markers, while the remaining markers on the model are as close as possible to the markers. So far, these are the only solutions we have found.

The manually derived initial guess on the segment lengths, joint axes of rotation as well as system coordinates at the first frame was fairly good, with values in the range of 1–7 cm from the finale values for the segment lengths and local marker coordinates for the optimised markers for the gait-optimised models. For the joint axes of rotation, we used the cadaver values as the initial guess. In the ROM optimised model, we used the finale values from the gait-optimised model with the ankle and subtalar joint axes fixed at the cadaver values as the initial guess. While these initial guesses were certainly very good, we did not attempt to systematically make the guess worse to determine when the solution could not be found.

Compared to a two-level optimisation approach (Reinbolt et al. 2005), the solution algorithm we presented requires much less computational effort although the solutions found from the two methods will be identical. The reason for this is that it is the same KKT conditions in Equation (13) that the two methods aim to solve, but the approach to finding the solution is different. In the two-level optimisation approach, once a set of system parameters is found in the outer level, a series of optimisation problems are solved to find the system coordinates at each sample. In Equation (13), that

corresponds to changing the system coordinates until L_{q_i} and L_{λ_k} are sufficiently close to zero for each sample by repeatedly calculating a search direction, a step length and updating the system coordinates. If a Newton-based method is used to find the search direction, this corresponds to solving Equation (16) multiple times. Once this has been done, a new search direction has to be found in the outer layer, which corresponds to solving Equation (17) with the current model parameters and system coordinates, determine a step length for the model parameters and then solve the inner layer optimisation problems again. This is repeated until Equation (13) is solved. To find the solution of an optimisation problem with a Newton method typically requires 2–30 iterations. In comparison, the solution method presented here requires a minimum of computational effort to find the search direction for the system coordinates. If all terms are re-used from the calculation of the search direction of the model parameters, the inner layer is reduced to a matrix-vector product and a vector subtraction per time step rather than multiple optimisation problems. The computational effort required to find the search direction for the model parameters is the same for both methods.

Although the presented method is much less computational expensive than the two-level optimisation method, more work is required before it is clinically applicable. Firstly, as with all local optimisation-based methods, the presented method requires a good initial guess, which we derived manually. In a clinical setting, an automatic method is required for this step. Secondly, determining which model parameters to optimise and which not to optimise is not a trivial task and requires a good understanding of the kinematical model as well as the task that is performed. In a clinical setting, a method to determine what can reliably be optimised has to be developed. Thirdly, when the model was optimised from the ROM trial, the algorithm required 5 h of computational time, which is impractical. The main contributors to this long computational time are the construction of the sums in Equation (17). An idea that has to be explored to overcome this computational barrier is to utilise more structure in the problem. For instance, in the current implementation, the sparsity in the linear equations in Equations (16) and (17) was not utilised. Additionally, when ROM is performed, motion of the joints is performed one at a time. However, when the model is optimised, all constant model parameters are part of the problem for all samples, even the parts of the motion, where the motion does not add information about a particular parameter. Therefore, in principle, it should be possible to determine when the motion adds more information to the determination of a parameter and eliminate the parameter from the problem in the parts of the motion, where little or no information is provided for it. Exploration of these possibilities is subject to current research.

References

Andersen MS, Damsgaard M, Rasmussen J. 2007. Construction of smooth time-varying weight functions to handle occasionally occluded markers in musculoskeletal models. In: Proceedings of the XIth international symposium on Computer Simulation in Biomechanics, Tainan, Taiwan.

Andersen MS, Damsgaard M, Rasmussen J. 2008. Kinematic analysis of over-determinate biomechanical systems. Comput Methods Biomech Biomed Eng. DOI: 10.1080/10255840802459412 (in press).

Ausejo S, Suescun A, Celigueta J, Wang X. 2006. Robust human motion reconstruction in the presence of missing markers and the absence of markers for some body segments. In: Proceedings of Digital Human Modeling for Design and Engineering Conference, Lyon, France.

Bell AL, Pedersen DR, Brand RA. 1990. A comparison of the accuracy of several hip center location prediction methods. J Biomech. 23:617–621.

Benoit DL, Ramsay DK, Lamontage M, Xu L, Wretenberg P, Renström P. 2006. Effect of skin movement artifact on knee kinematics during gait and cutting motions measured *in vivo*. Gait Posture. 24(2):152–164.

Bogert AJ, van den Smith GD, Nigg BM. 1994. *In vivo* determination of the anatomical axes of the ankle joint complex: an optimization approach. J Biomech. 27:1477–1488.

Boyd S, Vandenberghe L. 2004. Convex optimization. Cambridge: Cambridge University Press.

Charlton IW, Tate P, Smyth T, Roren L. 2004. Repeatability of an optimised lower body model. Gait Posture. 20(2):213–221.

Davis III RB, Õunpuu S, Tyburski D, Gage J. 1991. A gait data collection and reduction technique. Hum Mov Sci. 10:575–587.

Fregly BJ, Reinbolt JA, Rooney KL, Mitchell KH, Chmiclewski TL. 2007. Design of patient-specific gait modifications for knee osteoarthritis rehabilitation. IEEE Trans Biomed Eng. 54(9):1687–1695.

Klein Horsman MD, Koopman HFJM, van der Helm FCT, Prosé LP, Veeger HEJ. 2007. Morphological muscle and joint parameters for musculoskeletal modelling of the lower extremity. Clin Biomech. 22(2):239–247.

Leardini A, Cappozzo A, Catani, Toksvig-Larsen S, Petitto A, Sforza V, Cassanelli G, Giannini S. 1999. Validation of a functional method for estimation of hip joint centre location. J Biomech. 32:99–103.

Leardini A, Chiari L, Della Croce U, Cappozzo A. 2005. Human movement analysis using stereophotogrammetry. Part 3. Soft tissue artefact assessment and compensation. Gait Posture. 21(2):212–225.

Lu TW, O'Connor JJ. 1999. Bone position estimation from skin marker co-ordinates using global optimization with joint constraints. J Biomech. 32:129–134.

Nikravesh PE. 1988. Computer-aided analysis of mechanical systems. Englewood Cliffs, NJ: Prentice-Hall International, Inc.

Persson T, Lanshammar H, Medved V. 1995. A marker-free method to estimate joint centre of rotation by video image processing. Comp Meth Prog Biomed. 46:217–224.

Rasmussen J, de Zee M, Damsgaard M, Christensen ST, Marek C, Siebertz KA. 2005. A general method for scaling musculo-skeletal models. In: Proceedings of the international symposium on Computer Simulation in Biomechanics, Cleveland, OH, USA.

Reinbolt JA, Schutte JF, Fregly BJ, Koh BIL, Haftka RT, George AD, Mitchell KH. 2005. Determination of patient-

specific multi-joint kinematic models though two-level optimization. J Biomech. 38:621–626.

Reinbolt JA, Haftka RT, Chmielewski TL, Fregly BJ. 2008. A computational framework to predict post treatment outcome for gait-related disorders. Med Eng Phys. 30(4): 434–443.

Stagni R, Fantozzi S, Cappello A, Leardini A. 2005. Quantification of soft tissue artefact in motion analysis by combining 3D fluoroscopy and stereophotogrammetry: a study of two subjects. Clin Biomech. 20:320–329.

Vaughan CL, Davis BL, O'Connor JC. 1992. Dynamics of human gait. 2nd ed. Western Cape: Kiboho Publishers.